Impact of net metering programs on optimal load management in US residential housing – a case study

E. Georges[1]*, J. E. Braun[2], E. Groll[2], W. T. Horton[2], V. Lemort[1]

(1) Thermodynamics Laboratory, University of Liège, Liège, Belgium

(2) Ray W. Herrick Laboratories, Purdue University, West-Lafayette, Indiana, USA

1. ABSTRACT

In the US, buildings represent around 40% of the primary energy consumption and 74% of the electrical energy consumption (U.S. DOE, 2012). Incentives to promote the installation of on-site renewable energy sources have emerged in different states, including net metering programs. The fast spread of such distributed power generation represents additional challenges for the management of the electricity grid hence the interest in smart control of building loads and demand response programs.

This paper presents a study of a typical American house built in the 1990s in the Midwest and equipped with a single-speed air-to-air heat pump, an electric water heater and PV collectors. The study investigates the impact of different net metering tariffs on the optimal building electrical load management. The potential of load matching is characterized in terms of percentage of the electricity production consumed on-site and the proportion of the demand covered. Simulations are performed assuming perfect prediction of the electrical load profiles.

Results show a potential increase of load matching greater than 7% through control optimization with a suitable net-metering tariff. The associated cost saving for the consumer is about 10% greater compared to no optimization. Depending on the PV panel area, pay-back time increase due to lower buy-back tariffs can be reduced by 3 to 55% through optimal load matching.

Keywords: net metering, load matching, heat pump, electric water heater

2. INTRODUCTION

Since the late 1990s, many states in the US have started incentive programs to promote the installation of on-site renewable energy sources, such as tax incentives, low-interest loans and net energy metering. Net metering allows customers to supply their excess local electricity production to the electricity grid. These customers are often referred to as "prosumers". The introduction of such distributed electricity generation and fluctuating renewable energy complicate the planning and operation of the power system and may affect its reliability. At the distribution level, the main negative impacts are the overload of feeders and transformers, the risk of overvoltage and power quality disturbance (Bollen & Hassan, 2011). For example, Baetens et al. (2012) identified electrical challenges associated to the evolution of a neighborhood in Belgium composed of 33 detached residential houses towards net zero energy buildings (NZEBs) using heat pumps and building-integrated photovoltaic (PV) systems. Fraction of local PV supply wasted by inverter curtailing and peak transformer loads were quantified for different existing feeder strengths.

On-site generation can also help reduce the need for expansion and strengthening of transmission lines. In the residential sector, space heating and cooling and domestic hot water represent 72% of the energy consumption of a building (U.S. DOE, 2012). In the frame of this

work, heating and cooling needs are met through the use of a reversible heat pump and domestic hot water (DHW) is produced by an electric water heater. From an electricity grid system operator standpoint, such loads are identified as thermostatically controlled loads and represent a large potential for improvement of grid reliability through demand side management strategies (Kamgarpour et al., 2013). There are two ways for these buildings to interact with the electricity grid. On the one hand, they can offer flexibility (load shifting, peak shaving, etc.) in response to signals from the grid. On the other hand, if equipped with on-site generation, such as PV collectors, they can be used to diminish the impact of distributed energy production by promoting better load matching through load shifting. In both cases, these systems work in synergy to reduce the additional burden on the grid created by renewable energy generation (Sartori et al., 2012). Several studies have been performed both at the building and district levels. Arteconi et al. (2013) presented a study focusing on the influence of switching off a heat pump coupled to thermal energy storage during peak hours on the occupants' thermal comfort and on the electricity load curve in the UK context. D. Vanhoudt (2012) presented the results from lab tests of smart management strategies of a heat pump (with thermal storage for DHW and for space heating separately) in order to promote load matching with PV collectors. R. Shleicher-Tappeser (2012) considered different storage strategies between the production of electricity and the end-users in order to increase flexibility for power consumption. Main challenges associated to the consumer's behavior as well as to the development of incentives to develop new tariff structures were pointed out. De Coninck et al. (2013) investigated rule-based control strategies to shift heat pump operation for domestic hot water production to reduce curtailing losses in NZEBs neighborhood. Load shifting was initiated by different triggers: a given time frame, the power exchange with the grid or the voltage.

Another possibility to promote load shifting is through price signals from the electricity grid. In the US, net metering policies vary according to the states: so far, the excess power generation supplied to the grid is either "bought" at retail or at wholesale price tariffs (U.S. EIA, 2012). With the increase in the number of prosumers, electricity grid congestion and PV curtailment become more frequent, which restricts the amount of distributed power supplied to the grid. Such tariffs could become a direct reflexion of the level of saturation of the electricity grid. The purpose of this study is to evaluate the impact of different net metering tariffs as an incentive to increase load matching of on-site PV generation through optimal control of the domestic electrical load in the frame of demand-side management programs. The potential for load matching is characterized in terms of percentage of the electricity production consumed on-site and the proportion of the demand covered by decentralized electricity generation (Baetens et al., 2012 and Van Roy et al., 2013). Simulations are performed assuming perfect prediction of the electricity consumption profiles of the house. The newness of the study resides the assessment of the influence of such tariffs on the consumer's economic benefit through optimal load management.

In future work, stochastically generated load profiles will be introduced to take into account the uncertainty associated with occupants' behavior.

3. METHODOLOGY

3.1 Case studies

A typical 4-bedroom single-story ranch-type American house built in the 1990's is investigated (Figure 1). Building characteristics have been detailed by Holloway (2013). The building structure consists of a wood frame on a concrete ground floor. The 2-by-6 wood framing has been replaced by 2-by-4 construction, which is more common. The envelope insulation levels meet standard efficiency code (IECC, 2003) for the climate zone associated to the city of

Indianapolis in the Midwest (zone number 5, IECC 2009). Overall air-to-air heat transfer coefficients (U values) for walls, roof and windows are given in Table 1. Breakdown of the annual energy consumption is given in Figure 1.

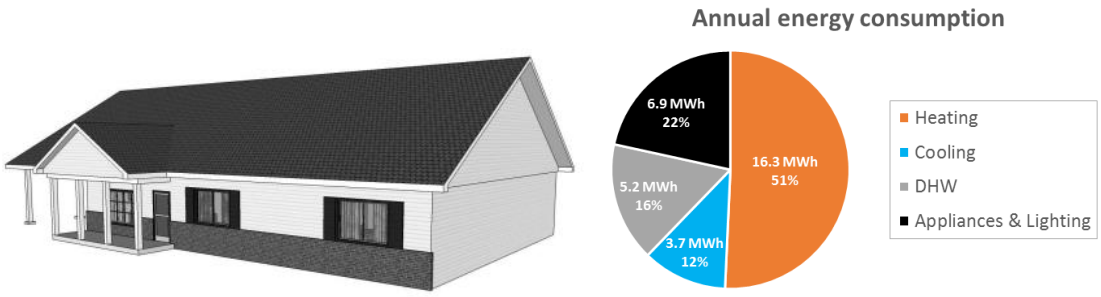

Figure 1: Left: Case study - Ranch house (Holloway, 2013) – Right: Breakdown of annual energy consumption

Table 1: Building envelope characteristics

	U values [W/m²K]
External walls	0.41
Roof	0.17
Windows	1.96

A detailed dynamic model of the house is available in TRNSYS (Holloway, 2013). Yearly simulation results were used to train a grey-box model that was implemented in the optimizer (see section 3.2.2). The grey-box model structure is illustrated in Figure 2. The model provides an accurate representation of the thermal response of the house at significantly reduced computational requirements. Root mean square error in free-floating zone temperature prediction was 0.18°C over a year for training data, and 0.19°C for the one-year validation data set.

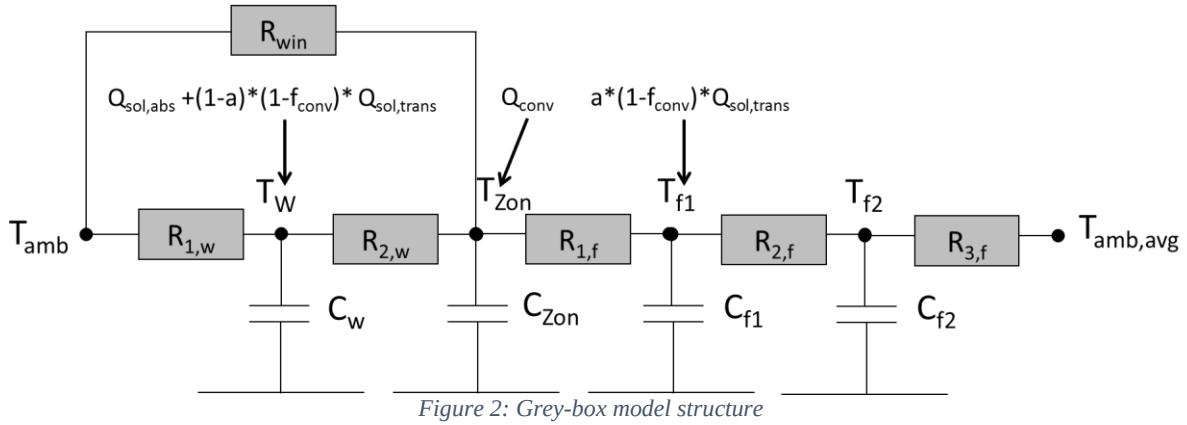

Figure 2: Grey-box model structure

The building is equipped with a reversible single speed air-to-air heat pump for space conditioning. It is modelled according to the ASHRAE toolkit model (Brandemuehl et al., 1993) in which capacity and coefficient of performance (COP) are defined as functions of their values at rated conditions (AHRI, 2008) and correction coefficients taking into account the dependency on the indoor and outdoor air temperatures and mass flow rates.

$$X = X_{rat} * f_{X_T} * f_{X_m}$$

$$f_{X_T} = a0 + a1 * T_{amb} + a2 * T_{amb}^2 + a3 * T_{Zon} + a4 * T_{Zon}^2 + a5 * T_{Zon} * T_{amb}$$

$$f_{X_m} = b1 + b2 * \dot{m}/\dot{m}_{rat}$$

All the coefficients for both COP and capacity were derived from performance maps for commercially available heat pumps (Holloway, 2013).

Domestic hot water production is ensured by an electric water heater equipped with two thermostats and two heating elements located in the upper third and in the lower two-thirds of the tank. Both heating elements can't be switched on simultaneously, and priority is given to the upper element. Hot water is drawn from the top of the tank and cold water is supplied at the bottom. The water in each part of the tank is assumed to be homogeneously mixed.

High efficiency photovoltaic panels are installed on the roof of the house. Two orientations are considered: south and west.

Table 2 summarizes the characteristics of each system.

Table 2: Systems characteristics summary for ranch-type house

	Systems characteristics – Ranch house	
Heat pump	Heating rated capacity / Rated COP (47°F/70°F)	8.33 kW / 3.85
	Cooling rated capacity / Rated COP (95°F/70°F)	8.03 kW / 3.41
	Back up electric heater	5 kW
Water heater	Volume	0.189 m³
	Lower / upper element heating power	4.5 kW / 4.5 kW
PV panel	Total area	20m² – 35m² – 50m²
	Rated power	4.3 kW_p – 7.5 kW_p – 10.75 kW_p
	Efficiency (PV manufacturer, 2014)	21.5%

3.2 Problem formulation

3.2.1 Net metering tariffs and cover factors

As already stated, net metering allows consumers to deliver surplus electricity generated on-site to the local distribution grid. Currently, in most states of the US, the tariff applied to this excess power generation is the retail tariff. From a customer's standpoint, this implies the same economic benefit whether the electricity produced by the PV system is consumed on-site or delivered to the grid. There is therefore no incentive to shift the electricity consumption in time to match the local production. With the increase in participation in electricity net-metering programs, this excess electricity released to the grid complicates the management of the electricity grid and can threaten its stability. Different net-metering tariffs are investigated here below.

To promote better load matching between production and consumption, four additional ratios of buy-back tariff (p_{PV}) to the retail tariff (p_{elec}) were considered:

- the excess power tariff is 75% of the retail tariff : $p_{PV}/p_{elec} = 0.75$
- the excess power tariff is 25% of the retail tariff : $p_{PV}/p_{elec} = 0.25$
- the excess power tariff follows a predetermined daily profile:
    - $p_{PV}/p_{elec} = 1$ during peak hours (7 to 9 am and 6 to 8 pm)
    - $p_{PV}/p_{elec} = 0.1$ during off-peak hours.

- the excess power buy-back tariff tends to zero : $p_{PV}/p_{elec} = 0.01$

The buy-back ratio is defined as p_{PV}/p_{elec}. It should be noted that the retail tariff p_{elec} chosen as reference is a flat tariff.

Load matching potential is determined by the following cover factors (Baetens et al., 2012):

- supply cover factor: represents the percentage of local electricity production consumed on-site:
$$\gamma_S = \frac{\sum \min(W_{cons.}, W_{PV})}{\sum W_{PV}} \quad (1)$$
- demand cover factor: represents the percentage of electricity consumption covered by on-site generation:
$$\gamma_D = \frac{\sum \min(W_{cons.}, W_{PV})}{\sum W_{cons.}} \quad (2)$$

3.2.2 Optimal response

Both water heater and grey-box building models can be represented by discrete state space formulations, and the overall system can be described by

$$\boldsymbol{x}(k+1) = \boldsymbol{A}\boldsymbol{x}(k) + \boldsymbol{B}\boldsymbol{u}(k) + \boldsymbol{E}\boldsymbol{w}(k)) \quad (3)$$

where $\boldsymbol{x}$ is the state space variable vector composed of the zone, wall, first and second floor temperature nodes, and top and bottom water tank temperature nodes:

$$\boldsymbol{x}^T = [T_{Zon}, T_W, T_{f1}, T_{f2}, T_{tank_{tp}}, T_{tank_{bt}}] \quad (4)$$

$\boldsymbol{u}$ is the vector of decision variables, namely the heat provided by the heat pump (or air-conditioning unit) to the house and the electric power supplied to the water heater:

$$\boldsymbol{u}^T = [Q_{house}, W_{WH,tp}, W_{WH,bt}] \quad (5)$$

and $\boldsymbol{w}$ is the vector of disturbances, i.e., the outdoor air temperature, the solar gains and the mains water temperature.

The methodology followed in this work consists in determining the optimal electrical consumption profile of the building in response to different net metering tariffs for a given prediction horizon. The cost function for this problem aims at minimizing the cost of electricity for the consumer, which is expressed by

$$Cost = \sum_{i=1}^{p} \left(\max(W_{cons.}(i) - W_{PV}(i), 0) - \max(W_{PV}(i) - W_{cons.}(i), 0) * \frac{p_{PV}}{p_{elec}} \right) \quad (6)$$

where p is the prediction horizon and the total electrical consumption $W_{cons.}$ is the sum of the power consumed by the heat pump (or air-conditioning unit), the auxiliary heater, the water heater and the appliances and lighting:

$$W_{cons.} = W_{HP/AC} + W_{WH,tp} + W_{WH,bt} + W_{aux.\ heater} + W_{appliances\ \&\ lighting} \quad (7)$$

Perfect predictions of the PV generation and of the use profiles for DHW, appliances and lighting are assumed (section 3.3). As for model predictive control methods, an optimal control response is obtained over the prediction horizon *p* and is applied to a defined control horizon *m* (with $m \leq p$). The prediction horizon is then shifted forward in time to the end of the control horizon, following a so-called "receding horizon" control scheme.

The following constraints should be satisfied:

- the building zone temperature should remain within a predefined dead band
$$T_{sp,low} \leq T_{Zon} \leq T_{sp,high} \quad (8)$$

with $T_{sp,low}$ and $T_{sp,high}$ set respectively to 20°C and 22°C in this case study.

- similarly, the water tank temperature in the upper and lower parts should remain within an imposed dead band:

$$T_{sp,low,DHW} \leq T_{tank,bt}, T_{tank,tp} \leq T_{sp,high,DHW} \quad (9)$$

with $T_{sp,low,DHW}$ and $T_{sp,high,DHW}$ set respectively to 35°C and 50°C in the bottom part and 50°C and 60°C in the top part of the tank.

- the heat delivered to/retrieved from the house should not exceed the full load capacity of the heat pump and auxiliary heater combined in heating mode or of the air-conditioning unit in cooling mode.
- similarly, the power supplied to the water tank should remain below the maximum value for each heating element, and both heating resistances can't work simultaneously.

The control of the HVAC systems is carried out following an "energy rate approach", which considers that the system is allowed to cycle freely to meet the energy requirement for a given simulation time step. Performance degradation due to cycling will be taken into account in future work.

The resulting minimization problem is a convex mixed linear integer programming problem and is solved with the open-source MATLAB compatible toolbox YALMIP (Löfberg, 2004) coupled to CPLEX solver (IBM, 2013).

3.3 Load profiles

The total building energy demand includes the building space heating (SH) and cooling (AC) loads, the domestic hot water needs and the electricity consumption of appliances and lighting. Water draw-off events as well as appliances and lighting use are modelled by predefined load profiles.

Realistically, it is not likely for the controller to have an exact prediction of the DHW, appliances and lighting events, since they directly relate to the unpredictable occupants' behavior. However, typical average load profiles are available and can be used for the prediction of the optimal response.

In the "Building America House Simulation Protocols", Wilson et al. (2014) provide a set of data including consumption and typical daily use profiles for an average American dwelling. Profiles for a four-bedroom/two-bathroom dwelling are illustrated in Figure 3. The DHW consumption includes hot water for baths, showers and sinks as well as a dishwasher and a clothes washer. The hot water daily consumption is 265 liters for weekdays and 290 liters on weekends at a supply temperature of 125°F (51.6°C). For lighting, a seasonal effect is taken into account. The annual electricity consumption for appliances and lighting is 6936 kWh.

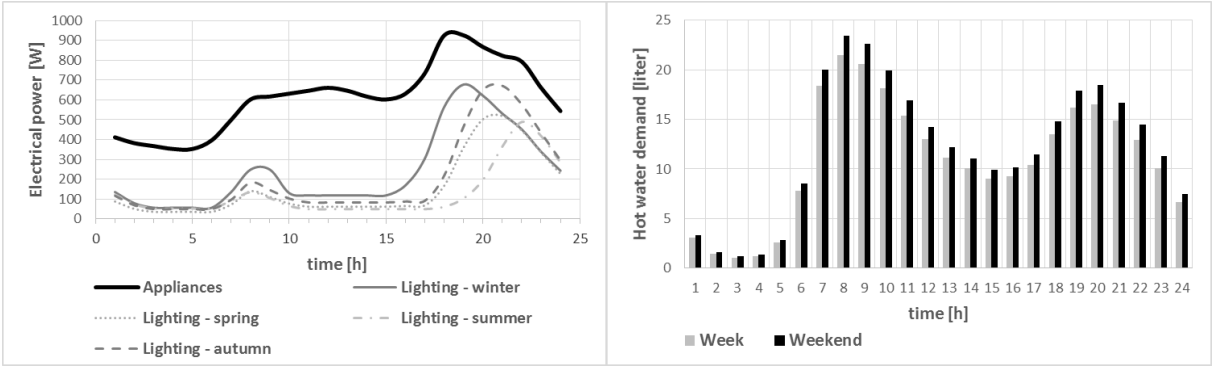

Figure 3: Average daily load profiles: Appliances and lighting (left) – DHW (right)

4. RESULTS AND DISCUSSION

The results presented in this section are obtained with optimal control, for a one-hour simulation time step, a prediction horizon of 24 hours and a control horizon of 12 hours for a year of simulation.

4.1 Influence of the net metering tariff

For the following results, a total surface of PV panels of 35m² was installed on the west slope of the roof, corresponding to a 30° tilt angle. The choice of orientation can be justified by the interest of a mid-afternoon peak PV production in the case of high peak electricity consumption in the evening. Five net-metering tariffs are investigated.

Results are presented in terms of demand and supply cover factors (section 3.2.1), total annual electricity consumption and cost saving for the consumer compared to the cost without PV collectors. They are summarized in Table 3. It should be noted that these results constitute an upper limit of the load matching potential, and that in practice, restrictions in the buy-back tariff may only apply during time-periods of grid congestion.

On a yearly basis, both demand and supply cover factors increase with lower surplus PV production tariff. When the electricity surplus sale price is reduced from 100% to 75% of the retail price, demand and supply cover factors increase by about 5% and 7% respectively. A less significant improvement (1% and 3%) is observed when reducing the tariff from 75% to 25%. The total cost saving for the consumer diminishes by 8% and 22% when the PV production buy-back price is reduced respectively from 100% to 75% and from 100% to 25%.

The results in terms of cover factors obtained with the variable tariff for peak and off-peak periods (predefined daily profile) are very similar to those obtained for a flat buy-back price of 25% of the retail price. For the present case study, with limited storage capacity, the values for the demand and supply cover factors tend to 0.37 and 0.57 respectively for a buy-back tariff approaching zero. A monthly analysis of the cover factors is illustrated in Figure 4. As expected, the demand cover factors are higher in the summer, whereas the supply cover factors are higher in the winter.

Despite the increase in on-site consumption of local electricity production with lower net-metering tariffs, the total electricity consumption cost for the consumer seems to increase. However, the cost saving should not be compared between the different tariffs. For the same tariff enforced by the electricity supplier, optimizing the consumer's load profile to match PV production brings about up to 10% additional cost saving compared to the cost without optimization.

Table 3: Supply/demand cover factors, total electricity demand and total cost for three net metering tariffs

	Optimal control				***No optimization***			***Comparison***
p_{PV} $/p_{elec}$	γ_D [ ]	γ_S [ ]	$W_{consumption}$ $[MWh/year]$	Cost saving [%]	γ_D [ ]	γ_S [ ]	Cost saving [%]	**Cost saving increase**
1	0.30	0.46	15.9	66.1	0.27	0.46	59.7%	**6.4%**
0.75	0.35	0.53	16.0	58.0	0.27	0.46	51.6%	**6.4%**
0.25	0.36	0.56	16.1	43.7	0.27	0.46	35.4%	**8.3%**
profile	0.36	0.54	16.1	43.1	0.27	0.46	34.4%	**8.7%**
0.01	0.37	0.57	16.2	37.4	0.27	0.46	27.6%	**9.8%**

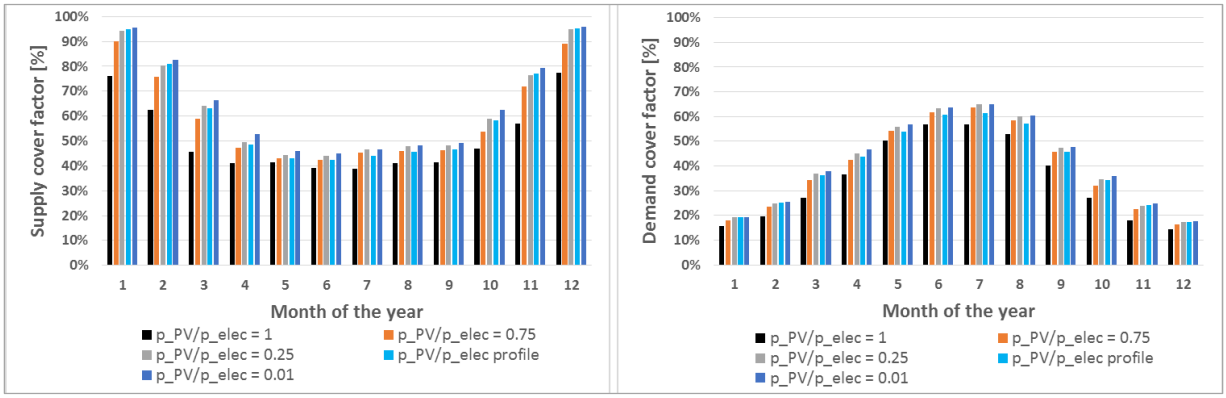

Figure 4: Demand and supply cover factors per month of the year.

Figure 5 and Figure 6 compare example optimal responses obtained for two buy-back tariffs: 100% and 25% of the retail price. As can be observed in Figure 5, for lower net-metering tariffs, the optimal control tends to shift the heat pump electrical demand to periods of time with simultaneous PV production. The building zone is preheated in order to lower the electricity consumption during periods of time with absence of sun. For the example highlighted in Figure 5, preheating the indoor air allows the heat pump to remain off for the next hour, and to work for shorter time periods the following two hours. An analogous trend is observed in Figure 6 for the electric water heater. Preheating the water typically allows for up to five-hour slowdown of the system.

The heating and cooling loads for space conditioning and the DHW heat load shifted towards sun production periods compared to the non-optimized heat load is illustrated in Figure 7 for two pay-back tariffs. The building structure provides a larger storage capacity in the winter. It should be noted that the values obtained are strongly dependent on temperature dead bands set as constraints, and would differ for a building with higher thermal inertia.

However, load shifting to increase load matching can lead to an increase in the total annual electricity consumption (Table 4). The slightly higher set points achieved increase the ambient heat losses and can slightly deteriorate the COP of the heat pump. Overconsumption of up to 2% were observed. One could argue that overconsumption could counter-balance the benefits retrieved from using on-site renewable electricity production in terms of CO2 emissions. In Indiana, in 2011, the electricity production mix was composed of 89% coal, 7% natural gas, 1% petroleum and 3% renewables (eia, 2011). Hourly CO2 emissions per MWh of electricity generated are illustrated in Figure *8* (OpenEI, 2011). Results in Table 4 show that despite overconsumption, increasing load matching allows to reduce CO2 emissions by up to 8.4%.

Finally, the optimal total electricity demand profile obtained with the time-varying net-metering pricing is illustrated in Figure 9. Load matching is enforced during off-peak hours, typically in the afternoon when the PV production is maximum. This also tends to shift part of the morning and night consumption peaks to off-peak periods, but not as significantly as for constant tariffs. Indeed, since surplus electricity production can be sold at a higher price during these periods, it remains interesting for the consumer to deliver electricity back to the grid. Therefore, flat tariffs seem more suitable as incentive for load matching.

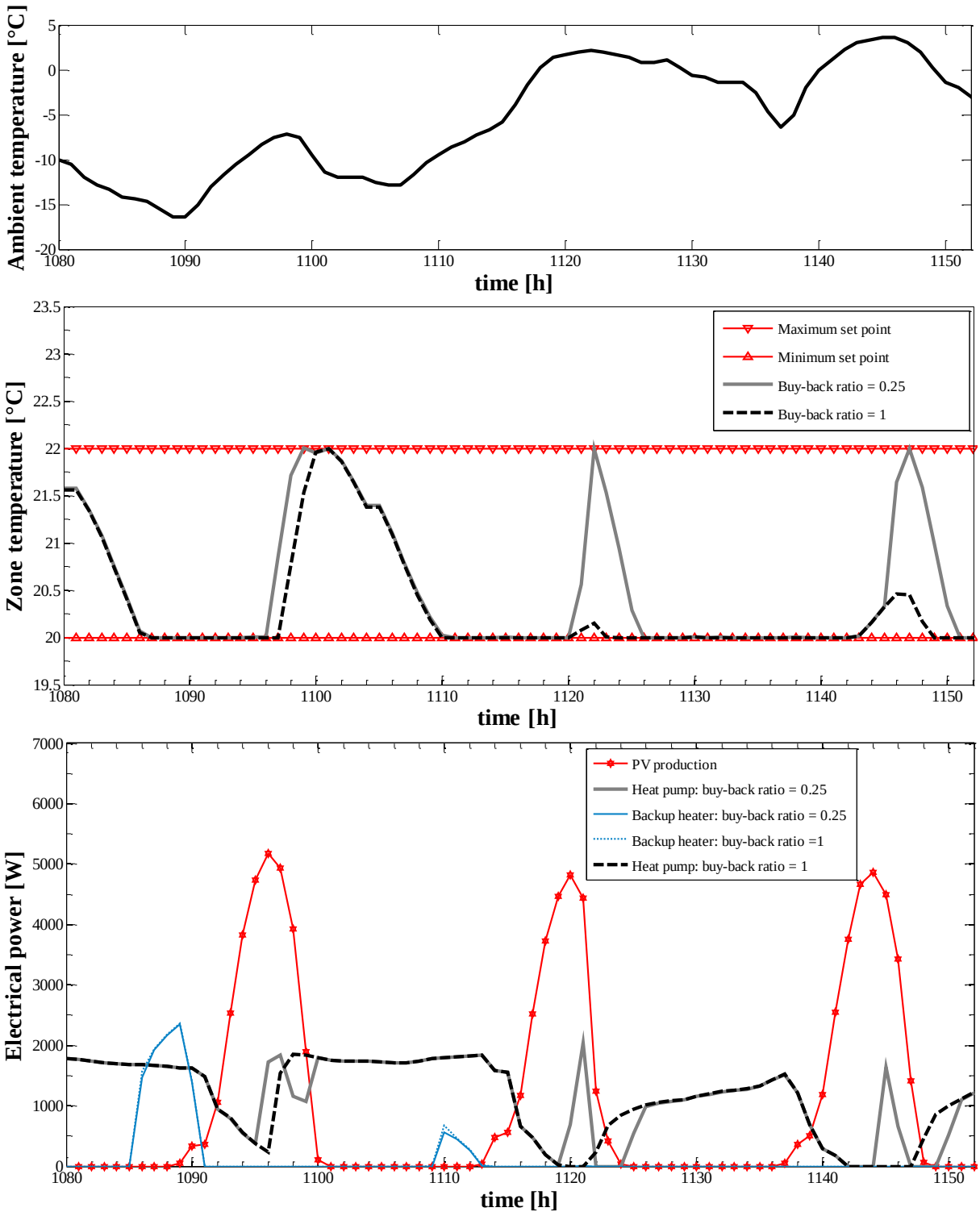

Figure 5: Bottom - Electrical power consumption for space heating for $p_{PV}/p_{elec}=1$ and $p_{PV}/p_{elec}=0.25$ and PV production for hours number 1080 to 1152 (February 14th to February 17th). Top – Corresponding zone and ambient temperatures.

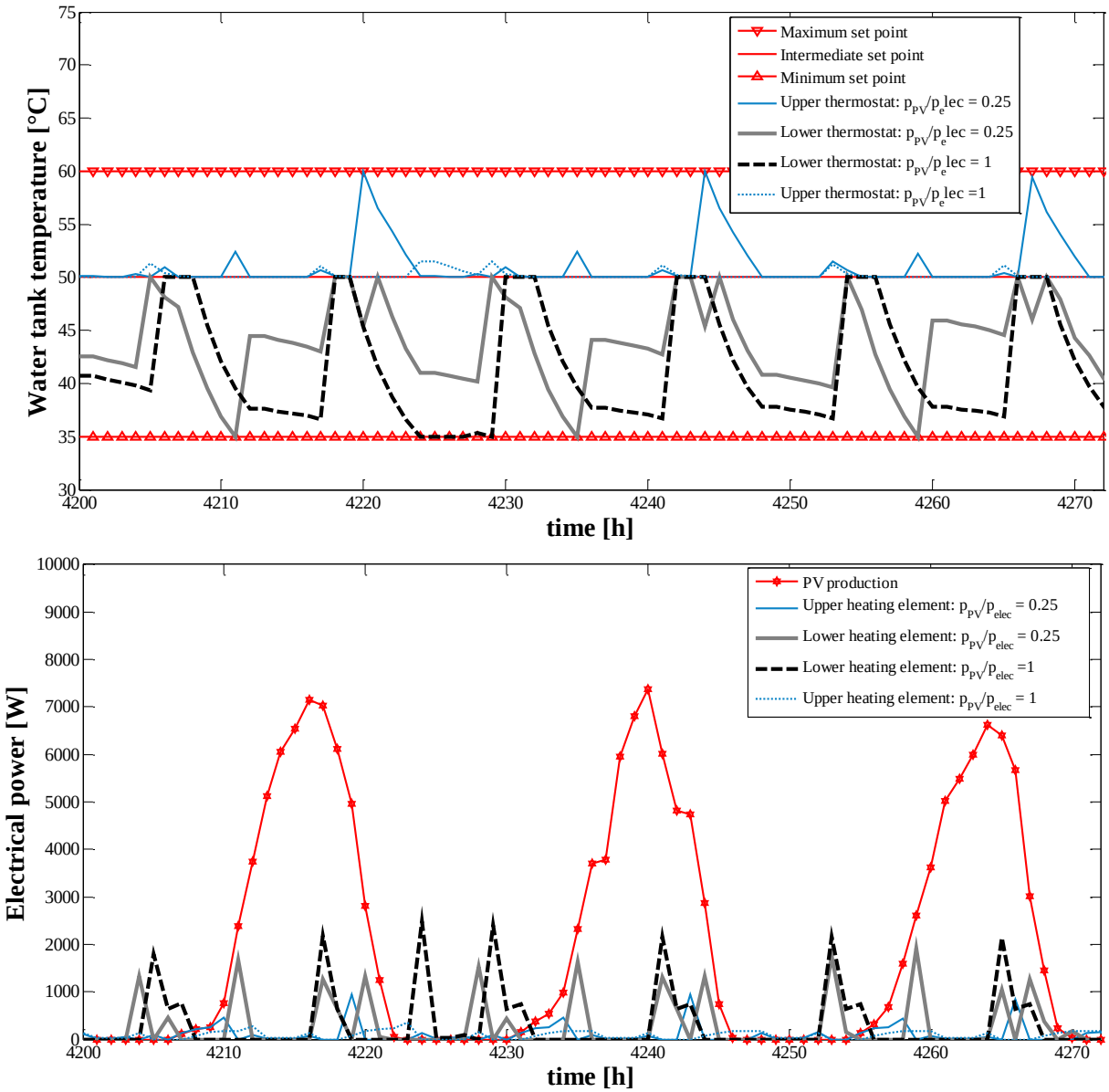

Figure 6: Bottom - Electrical power consumption for DHW for p_{PV}/p_{elec}=1 and p_{PV}/p_{elec}=0.25 and PV production for hours number 4200 to 4272(June 24th to June 27th). Top – Corresponding water tank lower and upper thermostat temperatures.

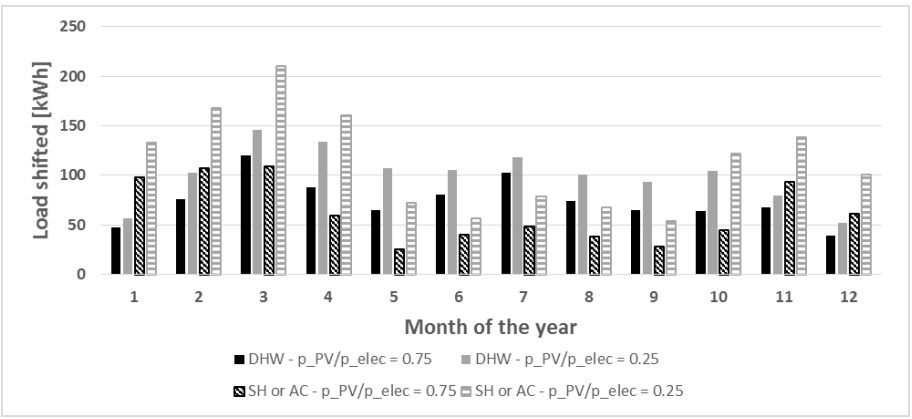

Figure 7: Thermal load shifted to match PV production per month for DHW and space heating or air-conditioning (SH or AC)

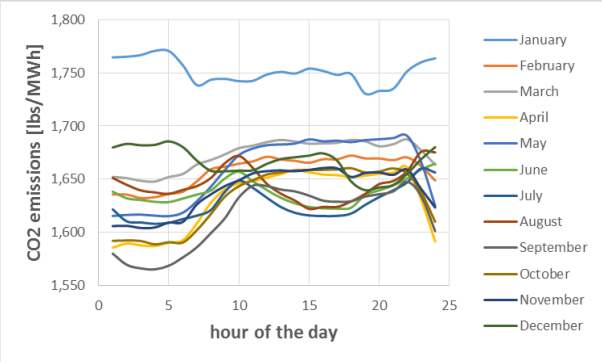

Figure 8: Average CO2 emissions per month in Indiana

Table 4: Over-consumption and CO2 emissions with optimal control

p_{PV}/p_{elec}	$W_{cons.}$ [MWh /year]	Over-consumption [%]	CO2 emissions [t]	**Reduction in CO2 emissions**
1	15.9	/	8.33	/
0.75	16.0	0.6	7.83	**6.0%**
0.25	16.1	1.1	7.65	**8.2%**
profile	16.1	1.1	7.77	**6.7%**
0.01	16.2	1.9	7.63	**8.4%**

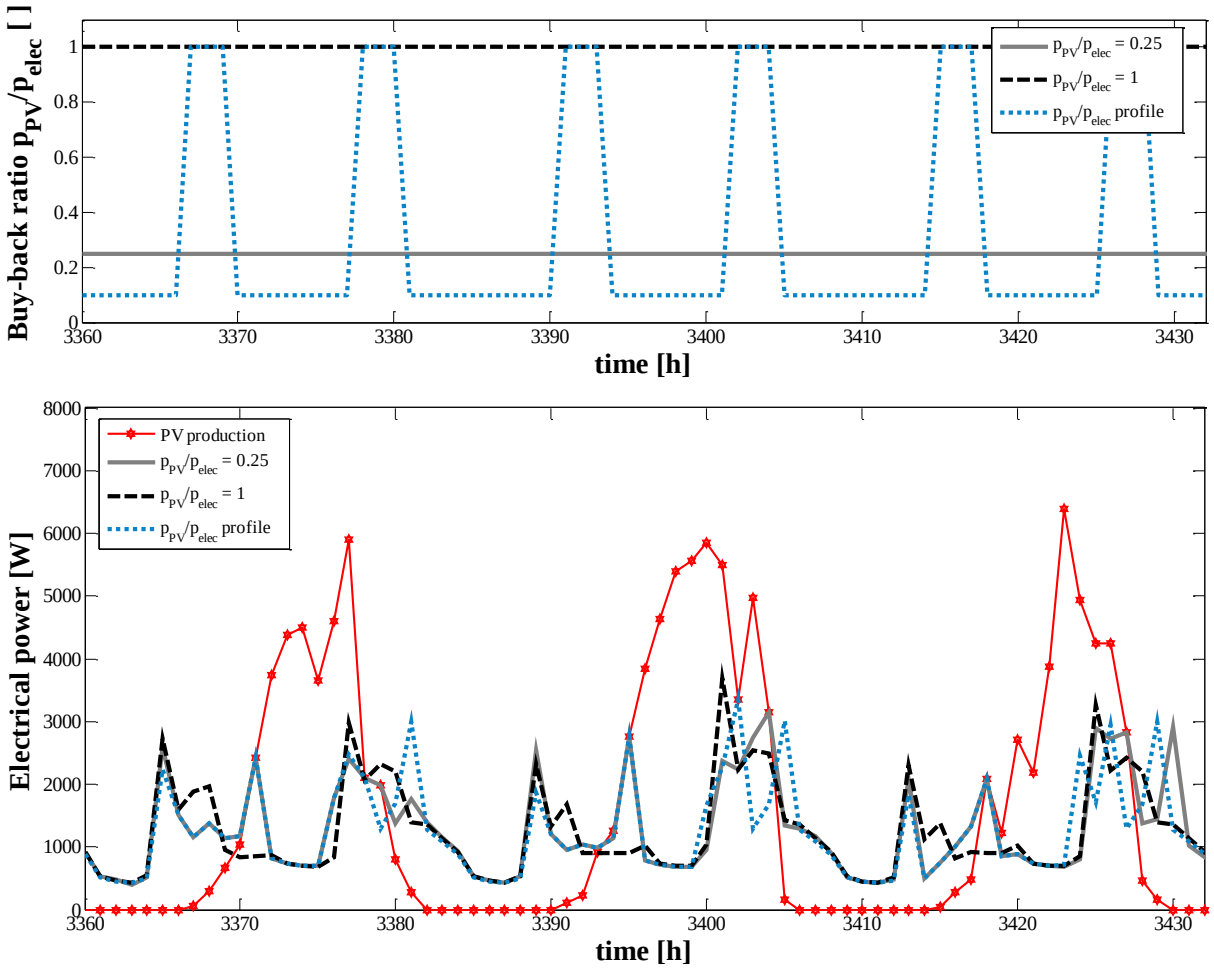

Figure 9: Comparison of total electricity consumption and PV production for p_{PV}/p_{elec} following a daily profile (1 during peak hours and 0.1 during off-peak hours), p_{PV}/p_{elec} =0.25 and p_{PV}/p_{elec} =1.

4.2 Influence of the PV panels orientation

In the previous section, the results were presented for 35m² of PV panels facing west. In this section, a comparison is presented with 35m² of south-oriented PV panels. The results given in Table 5 show an overall electricity demand coverage by on-site generation slightly larger (1%) with south-facing PV panels. Contrariwise, the proportion of electricity produced by the PV panels and consumed on-site is up to 7% greater for west orientation. This can be explained by the limited storage capacity of the building presented in this study and the existence of peak in electricity demand in the evening. Therefore, despite the lower total annual electricity production compared to south-oriented PV collectors, west facing PV panels seem more suitable to increase load matching in the case of low inertia buildings with peak electricity demand in the evening.

Table 5: Influence of PV panels orientation: west-facing and south-facing

	West-oriented PV		***South-oriented PV***	
p_{PV}/p_{elec}	γ_D [ ]	γ_S [ ]	γ_D [ ]	γ_S [ ]
1	0.30	0.46	0.31	0.40
0.75	0.35	0.53	0.36	0.46
0.25	0.36	0.56	0.38	0.49
profile	0.36	0.54	0.38	0.49
0.01	0.37	0.57	0.40	0.51

4.3 Influence of PV panel area

This section studies how the cover factors and consumer's pay-back time change with PV panels installed power for the different buy-back ratios. The total surface of PV panels was set respectively to 20m², 35m² and 50m². These areas correspond 38%, 66% and 94% coverage of the annual electrical consumption of the house.

The results obtained after optimization are summarized in Table 6. As expected, for approximately the same total electricity consumption, the demand cover factor increases with the surface area of PV panels. The same tariff incentive promotes load shifting to different extents depending on the PV area. For a buy-back ratio of 0.25, the supply cover factor reaches 0.80 for 20m² PV area, 0.57 for 35m² PV area and 0.45 for 50m² PV area. The proportion of electricity delivered to the distribution grid thus increases significantly with the PV area. This effect may seem negligible for a single house, but may affect the grid reliability at a neighbourhood scale.

Table 6: Comparison of supply/demand cover factors for different PV area and different buy-back ratios.

	PV Area = 20 m²		***PV Area = 35 m²***		***PV Area = 50 m²***	
p_{PV}/p_{elec}	γ_D [ ]	γ_S [ ]	γ_D [ ]	γ_S [ ]	γ_D [ ]	γ_S [ ]
1	0.24	0.64	0.30	0.46	0.34	0.36
0.75	0.28	0.74	0.35	0.53	0.38	0.41
0.25	0.29	0.78	0.36	0.56	0.40	0.43
0.01	0.30	0.80	0.37	0.57	0.41	0.45

In the US, the average installation cost of PV panels was 4.7$ per watt peak in 2013 (NREL, 2013). No significant scale benefits can be observed for an installed power in the range of 5kW$_p$ to 10 kW$_p$. A federal tax credit incentive provides 30% reduction of the cost for residential PV systems (IREC, 2012). Therefore, the installation costs are respectively 14150, 24675 and 35370 dollars for 20m², 35m² and 50m² PV areas. The electricity retail tariff for residential consumers in Indiana is 0.0945 $/kWh. The pay-back time for the consumer can be defined by the total installation cost divided by the annual cost saving.

Figure 10 (left) compares the consumer's pay-back time for optimized and non-optimized consumption profiles as a function of the buy-back ratio for different PV areas. The pay-back time increases significantly with decreasing buy-back ratios, and especially for larger PV areas. For buy-back ratios decreasing from 1 to 0.25, the pay-back time for non-optimized response increases by 36%, 69% and 93% respectively for 20m², 25m² and 50m² PV areas. Optimizing load profiles to match on-site PV production allows to reduce this increase by 16% to 19%. These results are in accordance with the evolution of the supply cover factors in Table 6.

Thus, for net-metering programs with buy-back tariffs lower than retail price and no other economic incentives, installing larger PV areas without increasing on-site storage capacity to promote load matching may become unprofitable. Given a life expectancy of about 30 years for PV panels, optimum sizing of PV panels, expressed in terms of percentage of the annual electricity consumption covered, can be derived for each buy-back ratio. Results are illustrated in Figure 10 (right). For a buy-back ratio of 1, there is no theoretical limit, and a maximum of PV panels should be installed. For buy-back ratios inferior to 1, the maximum coverage can be as low as 20% for non-optimized load profiles and 34% for optimized ones.

These conclusions are closely linked to net metering programs implemented in this study. The electricity supplier could promote other incentives in parallel, such as payoffs to prosumers who optimize on-site electricity consumption.

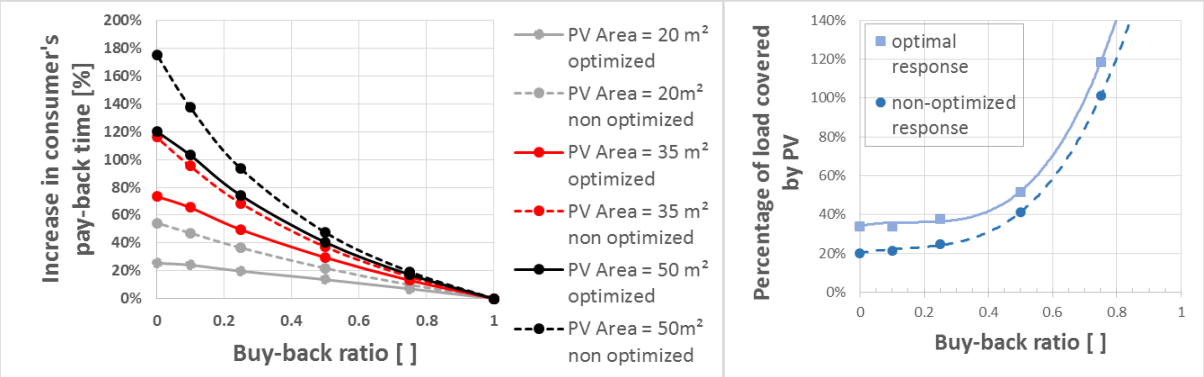

Figure 10: Left: Buy-back ratio as a function of p_{PV}/p_{elec} for three different total PV areas (20m², 35m² and 50m²) – Right: Optimal PV area expressed as a percentage of the annual load coverage vs buy-back ratio.

5. CONCLUSIONS

In this study, optimal management of the electricity demand of a typical US house equipped with a reversible heat pump, an electric water heater and PV panels has been investigated. The objective was to minimize the excess electricity production delivered to the grid by promoting on-site consumption through the use of different net metering tariffs.

Imposing a tariff lower than the retail tariff for the excess electricity generated proved to be a good incentive to promote load matching. Indeed, with 35 m² of PV panels on the west slope

of the roof and for a price set to 25% of the retail price, the yearly percentage of demand directly covered by on-site generation and the percentage of PV production consumed directly in the house increased by 6% and 9%. It was also shown that the increase in load matching is not proportional to the diminution in the tariff for a given installed PV power. Despite the increase in cover factors, the overall electricity cost for the consumer increases with a lower buy-back tariff. However, for the same tariff enforced by the electricity supplier, optimizing the consumer's load profile to match PV production brings about up to 10% additional cost saving compared to the cost without optimization, hence the interest in load-matching for both the consumer and the supplier. In terms of potential improvement in load matching, the choice of a flat tariff seems more suitable than a time-varying tariff.

With regard to PV panel orientation, it was shown that despite a lower total annual electricity production, west facing PV panels present supply cover factors up to 11% higher than south-facing ones and seem more suitable to promote load matching in the case of low inertia buildings with peak electricity demand in the evening.

Finally, for larger PV areas, reducing buy-back tariffs has a less significant impact on load matching improvement, and increases dramatically the consumer's pay-back time. For 50m² PV areas and non-optimized electricity load profiles, the pay-back time increases by up to 93% for pay-back ratios ranging from 1 to 0.25. Optimizing the load profile allows to reduce this increase by 19%. For 20m² PV area, the reduction in pay-back time reached up to 36%. Optimal percentage of installed load coverage were derived as a function of the buy-back ratio imposed.

In future work, the buy-back tariff could be adjusted to reflect the level of grid congestion. Other financial incentives from the electricity supplier could be investigated, such as complimentary payoffs for prosumers optimizing their load profiles to reduce their impact on the grid. Different heating and cooling schedules, such as night set-back strategies as well as different on-site storage capacities (higher thermal inertia buildings, complimentary hot water storage for space heating, etc.) will be studied. Finally the impact of the occupant's behavior will be introduced through stochastic load profiles for DHW draw-off events and appliances and lighting use.

REFERENCES

AHRI, 2008, *Performance Rating of Unitary Air-Conditioning & Air-Source Heat Pump Equipment*, No. 210/240-2008, 211 Wilson Boulevard, Suite 500, Arlington, VA 22201, USA.

Arteconi A., Hewitt N.J. and Polonara F., 2013, *Domestic demand-side management (DSM): Role of heat pumps and thermal energy storage (TES) systems*, Applied Thermal Engineering, vol. 51, 2013, pp. 155-165.

Baetens, R., De Coninck, R., Van Roy, J., Verbruggen, B., Driesen, J., Helsen, L., Saelens, D., 2012, *Assessing electrical bottlenecks at feeder level for residential net zero-energy buildings by integrated system simulation*, Applied Energy, vol. 96, pp. 74-83.

Bollen M., Hassan F., 2011, Integration of Distributed Generation in the Power System, 1st ed., John Wiley & Sons, IEEE press, Piscataway, NJ, USA.

Brandemuehl, M. J., Gabel, S., & Andresen, I., 1993. *HVAC 2 Toolkit: A Toolkit for Secondary HVAC System Energy Calculations*, Atlanta, Ga.: American Society of Heating, Refrigerating and Air-Conditioning Engineers.

De Coninck, R., Baetens R., Saelens, D., Woyte A. and Helsen L., 2013, *Rule-based demand side management of domestic hot water production with heat pumps in zero energy neighbourhoods*, accepted in Journal of Building Performance simulation.

eia Independent Statistics & Analysis - US. Energy Information Administration, 2011, *State Profiles and Energy Estimates*, http://www.eia.gov/state/seds/

Holloway, S., 2013, *An annual performance comparison of various heat pumps in residential applications*, PhD dissertation, Purdue University, IN, USA.

IBM ILOG, 2013, CPLEX Optimization Studio.

International Code Council. 2003, 2009, *International Energy Conservation Code (IECC)*.

Interstate Renewable Energy Council (IREC), 2012, *Database of State Incentives for Renewables and Efficiency (DSIRE) - Residential Renewable Energy Tax Credit.*

Kamgarpour M., Ellen C., Soudjani S. E. Z., Gerwinn S., Mathieu J. L., Müllner N., Abate A., Callaway D. S. Fränzle M., Lygeros J., 2013, *Modeling Options for Demand Side Participation of Thermostatically Controlled Loads*, IREP Symposium-Bulk Power System Dynamics and Control - IX, August 25-30, 2013, Rethymnon, Greece.

Löfberg J., 2004, *YALMIP: A Toolbox for Modeling and Optimization in MATLAB*, In Proceedings of the CACSD Conference, Taipei, Taiwan.

National Renewable Energy Laboratory (NREL), 2013, *The Open PV Project*, *https://openpv.nrel.gov/*

OpenEI, 2011, *Hourly Energy Emission Factors for Electricity Generation in the United States*, http://en.openei.org/datasets/dataset/hourly-energy-emission-factors-for-electricity-generation-in-the-united-states

Sartori I., Napolitano A., Voss K., 2012, *Net zero energy buildings: a consistent definition framework*, Energy and Buildings, vol. 48, pp. 220-232.

Shleicher-Tappeser R., 2012, *The building as system level for management and storage - electricity and heat storage in apartment and office buildings*, 7th International renewable Energy Storage Conference and Exhibition (IRES 2012), Berlin, November 12-14, 2012.

U.S. Department of Energy (DOE), 2012, *2011 Buildings energy data book*, Energy Efficiency & Renewable Energy.

U.S Energy Information Administration (EIA), 2012, *Policies for compensating behind-the-meter generation vary by State*, Today in Energy, May 9th, 2012.

Vanhoudt D. (VITO), 2012, *Lab test results of an active controlled heat pump with thermal energy storage for optimal integration of renewable energy*, 7th International renewable Energy Storage Conference and Exhibition (IRES 2012), Berlin, November 12-14, 2012.

Van Roy J., Salenbien R., Vanhoudt D., Desmedt J. and Driesen J., 2013, *Thermal and Electrical Cover Factors: Definition and Application for Net-Zero Energy Buildings*, in Proceedings of CLIMA 2013 Conference, Prague, Czech Republic, 16-19 June 2013.

Wilson E., Engebrecht Metzger, C., Horowitz S., Hendron R., 2014, *2014 Building America House Simulation Protocols*, National Renewable Energy Laboratory, Technical Report NREL/TP-5500-60988.

ACKNOWLEDGEMENTS

FNRS (Fond de la Recherche Scientifique) in Belgium is gratefully thanked for the funding of Emeline Georges as PhD research fellow.

NOMENCLATURE

Symbols		Subscripts	
C	thermal capacity	abs	absorbed
f	fraction	AC	air-conditioning
m	control horizon	amb	ambient
p	prediction horizon or price	avg	average
Q	heat transfer capacity	bt	bottom
R	thermal resistance	cons.	consumption
T	temperature	conv	convective
W	electrical power	D	demand (consumption)
X	capacity or COP	elec	electricity
		f	floor
		HP	heat pump
		m	mass flow rate
		p	peak
		rat	rated
		S	supply
		sol	solar
		sp	set point
		T	temperature
		tp	top
		trans	transmitted
		w	wall
		WH	water heater
		win	window
		Zon	zone